Article

Functional T cells are capable of supernumerary cell division and longevity

https://doi.org/10.1038/s41586-022-05626-9

Received: 1 July 2022

Accepted: 5 December 2022

Published online: 18 January 2023

Check for updates

Andrew G. Soerens[1], Marco Künzli[1], Clare F. Quarnstrom[1], Milcah C. Scott[1], Lee Swanson[1], JJ. Locquiao[1], Hazem E. Ghoneim[2], Dietmar Zehn[3], Benjamin Youngblood[4], Vaiva Vezys[1] & David Masopust[1]✉

Differentiated somatic mammalian cells putatively exhibit species-specific division limits that impede cancer but may constrain lifespans[1–3]. To provide immunity, transiently stimulated CD8$^+$ T cells undergo unusually rapid bursts of numerous cell divisions, and then form quiescent long-lived memory cells that remain poised to reproliferate following subsequent immunological challenges. Here we addressed whether T cells are intrinsically constrained by chronological or cell-division limits. We activated mouse T cells in vivo using acute heterologous prime–boost–boost vaccinations[4], transferred expanded cells to new mice, and then repeated this process iteratively. Over 10 years (greatly exceeding the mouse lifespan)[5] and 51 successive immunizations, T cells remained competent to respond to vaccination. Cells required sufficient rest between stimulation events. Despite demonstrating the potential to expand the starting population at least 10^{40}-fold, cells did not show loss of proliferation control and results were not due to contamination with young cells. Persistent stimulation by chronic infections or cancer can cause T cell proliferative senescence, functional exhaustion and death[6]. We found that although iterative acute stimulations also induced sustained expression and epigenetic remodelling of common exhaustion markers (including PD1, which is also known as PDCD1, and TOX) in the cells, they could still proliferate, execute antimicrobial functions and form quiescent memory cells. These observations provide a model to better understand memory cell differentiation, exhaustion, cancer and ageing, and show that functionally competent T cells can retain the potential for extraordinary population expansion and longevity well beyond their organismal lifespan.

The extent to which somatic mammalian cells can proliferate has been debated. Early reports that fetal chicken heart cells could grow in vitro for decades indicated that although organisms age, cells were immortal[7,8]. This sensationalistic experiment was not reproducible and attributed to cell transformation or continuous introduction of fresh cells[9]. The authors of ref. [10] putatively rejected diploid somatic cell immortality, reporting a division counter limiting human cells to 50–60 divisions. This is referred to as a 'Hayflick limit' and was ascribed to telomere shortening[3,11], proposed to reduce cancer but impose lifespan constraints, and species-specific in vitro cell division limits have been correlated with longevity (mouse cells undergoing fewer divisions and tortoise cells undergoing more)[2,12,13]. Species-specific lifespan limits may be intrinsic to other fundamental biological processes, including replication-dependent DNA mutations. For example, mice accumulate a similar number of DNA mutations per cell over their 3-year lifespan to that of humans over their 80-year lifespan, perhaps revealing a conserved lifespan-defining boundary[14]. Other impediments to cell longevity or proliferative potential include loss of proteostasis and metabolic fitness.

CD8$^+$ T lymphocytes can sustain quiescence for years, yet engage in a differentiation programme within minutes of activation, followed by accumulation of an unusual number of rapid cell divisions. Primary activated cells undergo a programmed burst of about 15–20 cell divisions, with the capacity for at least 3 cell divisions per day[15]. This results in massive clonal expansion and is the basis for the specificity and memory that typifies adaptive immunity. Whether cumulative T cell division potential is intrinsically finite or unlimited is relevant to control of chronic or recurring infections, cancer, vaccine boosting, age-associated immunologic senescence and adoptive cell therapies, as well as fundamental questions regarding mammalian cell biology.

Since the 1970s, there have been reports that T cells could occasionally be sustained in culture[16,17], although it has been debated whether this was the result of transformation[18], and the relevance of in vitro proliferation limits to organismal biology has been questioned[19,20]. Early attempts to grow anticancer T cells in vitro resulted in massive populations, but they survived poorly on transfer to patients[21–23]. This has been attributed to a lack of durable 'stemness' by T cells[24,25].

[1]Center for Immunology, Department of Microbiology and Immunology, University of Minnesota, Minneapolis, MN, USA. [2]Department of Microbial Infection and Immunity, College of Medicine, The Ohio State University, Columbus, OH, USA. [3]Division of Animal Physiology and Immunology, School of Life Sciences Weihenstephan, Technical University of Munich, Freising, Germany. [4]Department of Immunology, St. Jude Children's Research Hospital, Memphis, TN, USA. ✉e-mail: masopust@umn.edu

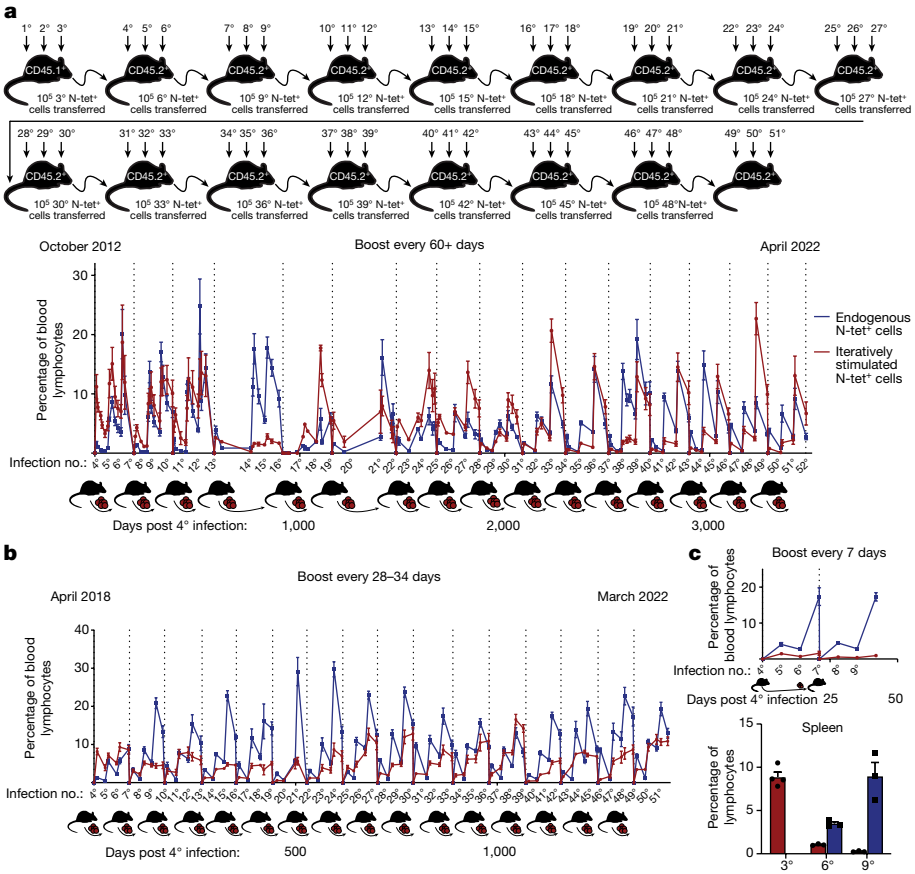

Fig. 1 | CD8$^+$ T cells can undergo seemingly unlimited bursts of proliferation if rested between stimulations. a, CD45.1$^+$ VSV/$N_{52–59}$-specific memory CD8$^+$ T cells were iteratively sorted, transferred to CD45.2$^+$ mice, and then boosted three times per mouse with 60+ days between each of three heterologous immunizations. The graph shows the percentage of total lymphocytes in blood that are comprised of transferred CD45.1$^+$ iteratively boosted cells (red) or newly generated CD45.2$^+$ recipient H-2K^b/$N_{52–59}$-specific cells (blue). N-tet$^+$ = H-2K^b/$N_{52–59}$-tetramer. **b**,**c**, As in **a**, except boosting was carried out at 28–34-day (**b**) or 7-day (**c**) intervals. Similar results were observed in trailing cohorts that have undergone 13, 21 or 31 (≥60-day interval), or 15 stimulations (28–34-day interval). **c** is representative of two experiments with similar results with $n = 4$ at 3° and $n = 3$ at 6° and 9°. Error bars show average and s.e.m. For flow cytometry gating strategies, see Supplementary Fig. 1. For exact number of mice at each time point in **a**,**b**, see Supplementary Table 1.

Antigen-experienced T cells that retain the ability to give rise to heterogenous daughter cells have been referred to as stem-like and provide more durable and expansible engraftment on transfer[26]. 'Memory stem cells' are typically described as sharing markers with naive T cells, including CD62L, although the property of unlimited division potential has not been tested[27]. Indeed, endogenous T cells responding to chronic infections or cancer undergo progressive in vivo 'exhaustion', defined by impaired proliferative ability, loss of potential to express effector cytokines and failure to eliminate immune targets[6]. When resting memory T cells have been serially passaged and stimulated with transient infections in vivo, they failed to respond to further stimulation within 4–7 generations[4,28,29]. These data support a model in which T cells have an intrinsic limit to their proliferation capacity, whether the antigen stimulation is chronic or periodic; however, this result may have depended on specific experimental conditions[30].

Proliferation and longevity potential

We wished to test whether: senescence, exhaustion and death are inevitable consequences of cumulative stimulations, divisions or species lifespan constraints; or T cells have the intrinsic potential to expand indefinitely. We designed an experiment that could isolate the potentially different effects of chronic versus cumulative stimulation, supersede species lifespan limits and permit iteratively potent CD8$^+$ T cell boosts by overcoming neutralizing antibody interference and competition for antigen by abundant memory T cell populations. CD45.1$^+$ C57Bl/6 female mice were immunized with three heterologous prime–boost immunizations (vesicular stomatitis virus subtype New Jersey (VSVnj); vaccinia virus expressing the VSV Indiana (VSVind) nucleoprotein (VVn); and VSVind (see Methods)) at ≥60-day intervals, which results in an abundantly expanded and long-lived 3° memory CD8$^+$ T cell population specific for the '$N_{52–59}$' peptide of VSV[30]. H-2K^b/$N_{52–59}$ major histocompatibility complex I tetramer$^+$CD8$^+$ T cells were then sorted from spleen and lymph nodes and 1×10^5 were transferred to congenic CD45.2 recipients, which subsequently received three additional immunizations (4° VSVind, 5° VVn and 6° VSVnj) at ≥60-day intervals. Although C57Bl/6 female mice survive only up to about 1,100 days[5], we were able to continue this sorting–transfer–three-immunization process for about 10 years totalling 51 cumulative immunization events because the CD45.1$^+$ population never lost the ability to expand following immunization (Fig. 1a). These cells also populated nonlymphoid tissues (Extended Data Fig. 1). These data showed that T cell expansion potential is not limited by the age of the origin population or the number of stimulation events.

We then tested whether an interval of ≥60 days was required between boosts[31]. Vaccinations, cell sorting and transfers were carried out as in Fig. 1a, except with 28–34 days between each immunization. We observed no substantive loss of continued expansibility through 51 stimulations (Fig. 1b). However, boosting every 7 days resulted in rapid deterioration of expansion potential (Fig. 1c). Collectively, these data

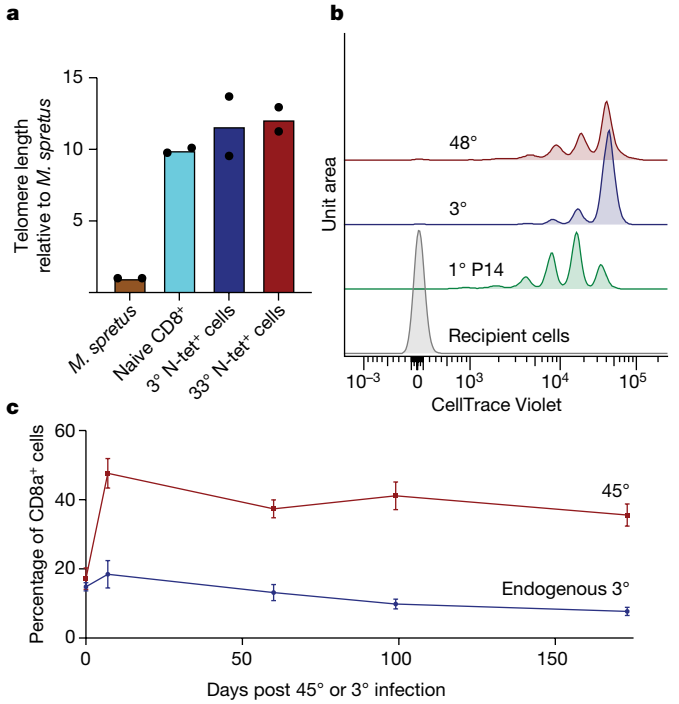

Fig. 2 | Iteratively boosted T cells maintain telomere length, cell cycle control and durability. a, Naive, 3° memory or 33° memory CD8$^+$ T cells were sorted, and then tested for telomere length by quantitative PCR and compared to *Mus spretus* reference DNA. **b**, 3° and 48° cells were labelled with CellTrace Violet division-tracking dye, and then transferred to recipients without further boosting. Primary lymphocytic choriomeningitis virus (LCMV)-specific P14 memory CD8$^+$ T cells were transferred for comparison. Cumulative cell divisions, indicated by dye dilution, were evaluated in spleen 34 days later. **c**, 45° and endogenous 3° memory CD8$^+$ T cells were tracked in blood for 173 days following infection. **a**–**c** are representative of two experiments with similar results, $n = 2$ (**a**), $n = 4$ (**b**), $n = 5$ (**c**). Error bars show average and s.e.m. For flow cytometry gating strategies, see Supplementary Fig. 2.

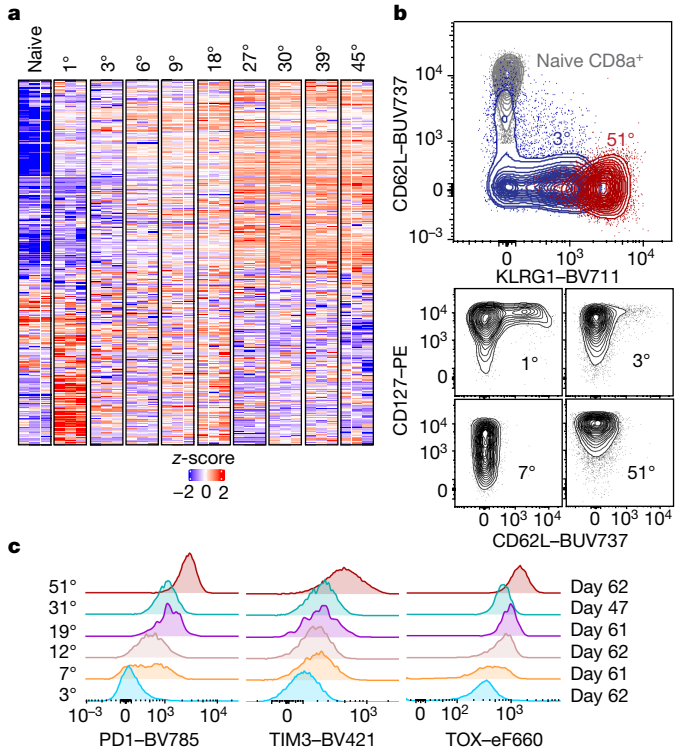

Fig. 3 | Iterative boosting induces progressive changes in gene and protein expression and acquisition of exhaustion markers. a, RNA-seq was carried out on naive and N-specific memory CD8$^+$ T cells that had experienced progressive boosts. Shown is a heatmap of the genes that were previously reported[42] to be uniquely expressed by exhausted CD8$^+$ T cells. **b**,**c**, The phenotype of naive and various generations of H-2K^b/N$_{52–59}$-specific memory cells isolated from blood was assessed by flow cytometry. All samples were run on the same day from staggered cohorts. The right column in **c** indicates days after last boost. **a**, $n = 3$ per group. **b**,**c**, Representative of $n = 3$ (7°), $n = 4$ (3°, 12°, 19° and 31°) or $n = 9$ (51° and naive), from at least two independent experiments with similar results. For flow cytometry gating strategies, see Supplementary Fig. 3.

indicate that although iterative stimulation can result in senescence or death among T cells, this fate is not a biological imperative.

Cell cycle integrity

It has been proposed that cell proliferation is accompanied by telomere shortening that induces cellular senescence, prevents cancer and limits lifespan. Some have questioned this paradigm[19,32,33], and many dividing cells, including activated T cells, express telomerase[34–36]. As we observed >50 bursts of substantial proliferation among a T cell population that has outlived its species, we examined telomere length by quantitative PCR[37]. Telomere length was maintained (Fig. 2a). Iterative transfers would seemingly select for cancer cells that outgrow untransformed cells. We loaded iteratively stimulated T cells (ISTCs) with a cell-tracking dye, and then transferred them to mice without subsequent stimulation. Thirty-four days later, we found no evidence that ISTCs lost growth control; indeed, they underwent less homeostatic turnover than primary memory cells (Fig. 2b). Moreover, although the ISTC population was durable, it was not inflationary (Fig. 2c). Thus, memory T cells can accumulate many divisions over many years without malignant transformation or loss of durability.

Phenotypic evolution

Early claims of immortal propagation of untransformed cells were later attributed to continuous seeding with young cells[9]. We addressed this possibility by sorting ISTCs before every transfer on a genetically encoded marker combination unique to the primary immunized mouse (CD45.1$^+$CD45.2$^-$; Fig. 1a). Furthermore, boosting was associated with progressive changes in gene expression, ruling out contamination with a dominant young T cell population (Fig. 3a and Extended Data Fig. 2). Changes were also observed at the protein level. ISTCs did not resemble phenotypes associated with central or stem memory T cells that preponderate primary immune responses as they lacked CD62L and expressed the 'senescence marker' KLRG1 (Fig. 3b). Moreover, each generation progressively acquired molecules thought to define T cell exhaustion, including PD1, TIM3 (also known as HAVCR2) and TOX (Fig. 3c).

Maintenance of immunological functions

PD1 is expressed in response to recent T cell receptor stimulation and is maintained by chronic antigen stimulation[38]. As antigen is not known to persist after this vaccination regimen, we tested whether PD1 expression was epigenetically maintained after iterative acute boosts. When ISTCs rested in recipient mice for >300 days after a single boost, they still maintained PD1 whereas endogenous primary memory CD8$^+$ T cells specific for the same antigen within the same mouse lacked PD1 (Fig. 4a). We also observed that CpG dinucleotides within the *Pdcd1* locus had become demethylated and that chromatin had become accessible (Fig. 4b,c). These data indicated that ISTCs phenocopied exhausted T cells exposed to chronic antigen, but the underlying regulation may be different. RNA sequencing (RNA-seq) and flow cytometric analyses revealed that ISTCs only partly acquire

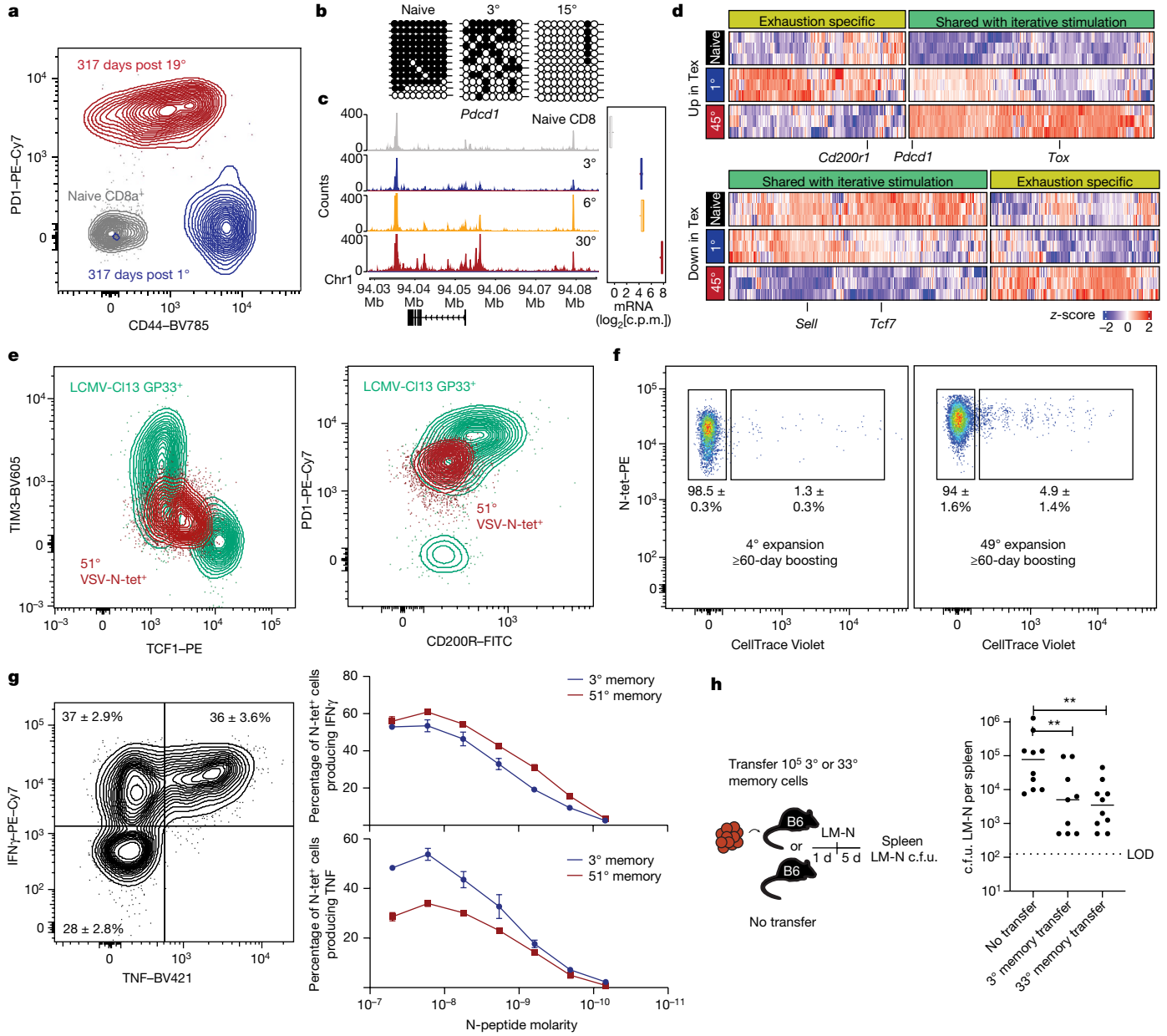

Fig. 4 | Transcriptional, epigenetic and functional profiling distinguishes ISTCs from exhausted T cells. a, 18° CD45.1$^+$ ISTCs were transferred to naive mice before a single immunization with VSVind. 317 days later, ISTCs and endogenous VSV/$N_{52–59}$-specific primary memory and naive CD8$^+$ T cells were assessed for maintenance of PD1 expression in blood. **b**,**c**, Methylation (**b**) or chromatin accessibility (**c**) of the *Pdcd1* locus (encoding PD1) was evaluated in naive, 3° or ISTC cells by bisulfite sequencing or assay for transposase-accessible chromatin using sequencing (ATAC-seq), respectively. *Pdcd1* RNA as measured by RNA-seq is also shown. Mb, megabase. **d**, Gene expression modules that are shared or unshared with genes reported to be upregulated or downregulated by exhausted CD8$^+$ T cells (Tex)[42]. **e**, Spleens with GP33-specific cells induced by chronic LCMV clone 13 (Cl13) or ISTCs were analysed by flow cytometry. **f**, 3° or 48° cells were labelled with CellTrace Violet division-tracking dye and transferred to recipients that were then infected with VSVind. The plots show cell division indicated by CellTrace Violet dilution 16 days after booster immunization. **g**, IFNγ and TNF staining 4 h after peptide stimulation. Representative flow cytometry (left panel) and response to peptide titration (right graphs). **h**, ISTCs or endogenous VSV/$N_{52–59}$-specific 3° memory cells were transferred to naive mice, which were then infected intravenously with *Listeria monocytogenes* expressing VSV-N (LM-N), and then assessed five days (5 d) later for bacterial burden in spleen. c.f.u., colony-forming units; LOD, limit of detection. $n = 3$ (**a**,**c**,**d**,**g**), $n = 4$ (**b**,**e**), $n = 4$ (4°) or 5 (49°) (**f**), $n = 9$ (3°) or 10 (no transfer and 33°) (**h**). **a**,**e**–**g** are representative of ≥2 similar experiments, **b**–**d** show data from a single experiment. **g** shows data combined from two experiments. Ordinary one-way analysis of variance with Dunnett's multiple-comparison test was used on $\log_{10}$-transformed data to test for significance between groups; $^{**}P = 0.0086$ (for 3°) or $P = 0.0028$ (for 33°). Error bars show average and s.e.m. For flow cytometry gating strategies, see Supplementary Fig. 4. See Supplementary Information 3 for full statistical test details.

the exhaustion programme described for chronic viral infection in mice (Fig. 4d,e). ISTCs differed from exhausted T cells because they maintained the capacity to proliferate in response to antigen (Fig. 1). Indeed, when we transferred CellTrace Violet-labelled 3° and 48° ISTCs, a similar proportion of cells underwent ≥8 divisions following a single additional boost (Fig. 4f). Moreover, ISTCs did not lose the ability to produce interferon-γ (IFNγ) and substantial tumour necrosis factor (TNF) effector cytokines within 4–5 h of ex vivo peptide stimulation (Fig. 4g), nor were they diminished in the ability to control a microbial infection (Fig. 4h).

Discussion

These data demonstrate that T cells intrinsically have the capacity for seemingly unlimited population expansion and substantially outliving their host organism. Whether other somatic cells also exhibit this potential is unknown. Unexpectedly, we failed to capture ISTCs that detectably lost proliferation control, raising questions of whether antigen-experienced T cells are particularly poised to trigger cell death in response to pre-transformation events. This biology may accommodate the unusual lifestyle of T cells, characterized by long periods of quiescence punctuated by rapid bursts of extensive proliferation, and then programmed death of most of the expanded population. Perhaps ISTCs could help inform the biology of protection from cancer as well as maintaining cellular fitness far beyond the perceived constraints of time and experience.

Nevertheless, ISTCs changed epigenetically, transcriptionally and phenotypically with time and stimulation history. They lost canonical markers associated with memory T cell 'stemness'[27] and acquired markers associated with T cell exhaustion and dysfunction[6] (Fig. 3). Although they do not seem to expand equivalently to naive or central memory T cells on a per cell basis (Fig. 1a), progressive phenotypic changes in ISTCs were not parallelled by any detectable cumulative erosion in abilities to proliferate or form durable memory over the final 48 boosts (Fig. 2c). Our results do not reject the concept of T cell stemness, but dissociate self-renewing potential from markers previously associated with the ability to maintain longevity and proliferative fitness. ISTCs also dissociate exhaustion, as defined by proliferative ability, function and antigen-independent longevity, from phenotypes common to exhausted cells characterized in chronic infection or cancer. Functional $PD1^+$ T cells have also been observed in humans, and these may represent cells that have undergone iterative stimulation through heterosubtypic reinfections or pathogen recrudescence[39,40].

T cell senescence, exhaustion or death is frequently observed in settings of chronic stimulation, extremes of age and certain models of iterative stimulation punctuated by intervening rest[4,6,28–30,41]. Our results indicate that these fates are avoidable. Indeed, because ISTCs were diluted before every three boosts, a conservative estimate indicates that, on average, each of the approximately 200 $H\text{-}2K^b/N_{52–59}$-specific naive $CD8^+$ T cells present within unimmunized mice had the proliferative potential to give rise to more than 10^{41} 51^o resting memory $CD8^+$ T cells (Extended Data Fig. 3), with a total cell volume of more than 30,000 times that of planet Earth. ISTCs provide a model to dissect the parameters that permit everlasting proliferative capacity and longevity among T cells, as well as the broader underlying biological mechanisms of maintaining fitness.

Online content

Any methods, additional references, Nature Portfolio reporting summaries, source data, extended data, supplementary information, acknowledgements, peer review information; details of author contributions and competing interests; and statements of data and code availability are available at https://doi.org/10.1038/s41586-022-05626-9.

1. Stanley, J. F., Pye, D. & MacGregor, A. Comparison of doubling numbers attained by cultured animal cells with life span of species. *Nature* **255**, 158–159 (1975).
2. Röhme, D. Evidence for a relationship between longevity of mammalian species and life spans of normal fibroblasts in vitro and erythrocytes in vivo. *Proc. Natl Acad. Sci. USA* **78**, 5009–5013 (1981).
3. Bodnar, A. G. et al. Extension of life-span by introduction of telomerase into normal human cells. *Science* **279**, 349–352 (1998).
4. Masopust, D., Ha, S.-J., Vezys, V. & Ahmed, R. Stimulation history dictates memory CD8 T cell phenotype: implications for prime-boost vaccination. *J. Immunol.* **177**, 831–839 (2006).
5. Kunstyr, I. & Leuenberger, H. G. Gerontological data of C57BL/6J mice. I. Sex differences in survival curves. *J. Gerontol.* **30**, 157–162 (1975).
6. McLane, L. M., Abdel-Hakeem, M. S. & Wherry, E. J. CD8 T cell exhaustion during chronic viral infection and cancer. *Annu. Rev. Immunol.* **37**, 457–495 (2019).
7. Carrel, A. On the permanent life of tissues outside of the organism. *J. Exp. Med.* **15**, 516–528 (1912).
8. Ebeling, A. H. A ten year old strain of fibroblasts. *J. Exp. Med.* **35**, 755–759 (1922).
9. Witkowski, J. A. Dr. Carrel's immortal cells. *Med. Hist.* **24**, 129–142 (1980).
10. Hayflick, L. & Moorhead, P. S. The serial cultivation of human diploid cell strains. *Exp. Cell Res.* **25**, 585–621 (1961).
11. Allsopp, R. C. et al. Telomere length predicts replicative capacity of human fibroblasts. *Proc. Natl Acad. Sci. USA* **89**, 10114–10118 (1992).
12. Goldstein, S. Aging in vitro growth of cultured cells from the Galapagos tortoise. *Exp. Cell Res.* **83**, 297–302 (1974).
13. de Magalhães, J. P. & Toussaint, O. Telomeres and telomerase: a modern fountain of youth? *Rejuv. Res.* **7**, 126–133 (2004).
14. Cagan, A. et al. Somatic mutation rates scale with lifespan across mammals. *Nature* **604**, 517–524 (2022).
15. Boer, R. J. D., Homann, D. & Perelson, A. S. Different dynamics of CD4+ and CD8+ T cell responses during and after acute lymphocytic choriomeningitis virus infection. *J. Immunol.* **171**, 3928–3935 (2003).
16. Morgan, D. A., Ruscetti, F. W. & Gallo, R. Selective in vitro growth of T lymphocytes from normal human bone marrows. *Science* **193**, 1007–1008 (1976).
17. Gillis, S. & Smith, K. A. Long term culture of tumour-specific cytotoxic T cells. *Nature* **268**, 154–156 (1977).
18. Effros, R. B., Dagarag, M., Spaulding, C. & Man, J. The role of CD8+ T-cell replicative senescence in human aging. *Immunol. Rev.* **205**, 147–157 (2005).
19. Rubin, H. The disparity between human cell senescence in vitro and lifelong replication in vivo. *Nat. Biotechnol.* **20**, 675–681 (2002).
20. Akbar, A. N. & Henson, S. M. Are senescence and exhaustion intertwined or unrelated processes that compromise immunity? *Nat. Rev. Immunol.* **11**, 289–295 (2011).
21. Rosenberg, S. A. et al. Use of tumor-infiltrating lymphocytes and interleukin-2 in the immunotherapy of patients with metastatic melanoma. *N. Engl. J. Med.* **319**, 1676–1680 (1988).
22. Rosenberg, S. A. et al. Treatment of patients with metastatic melanoma with autologous tumor-infiltrating lymphocytes and interleukin 2. *J. Natl Cancer Inst.* **86**, 1159–1166 (1994).
23. Dudley, M. E. & Rosenberg, S. A. Adoptive-cell-transfer therapy for the treatment of patients with cancer. *Nat. Rev. Cancer* **3**, 666–675 (2003).
24. Zhang, Y., Joe, G., Hexner, E., Zhu, J. & Emerson, S. G. Host-reactive CD8+ memory stem cells in graft-versus-host disease. *Nat. Med.* **11**, 1299–1305 (2005).
25. Gattinoni, L. et al. Wnt signaling arrests effector T cell differentiation and generates CD8+ memory stem cells. *Nat. Med.* **15**, 808–813 (2009).
26. Gattinoni, L. et al. A human memory T cell subset with stem cell–like properties. *Nat. Med.* **17**, 1290–1297 (2011).
27. Graef, P. et al. Serial transfer of single-cell-derived immunocompetence reveals stemness of CD8+ central memory T cells. *Immunity* **41**, 116–126 (2014).
28. Wirth, T. C. et al. Repetitive antigen stimulation induces stepwise transcriptome diversification but preserves a core signature of memory CD8+ T cell differentiation. *Immunity* **33**, 128–140 (2010).
29. Rai, D., Martin, M. D. & Badovinac, V. P. The longevity of memory CD8 T cell responses after repetitive antigen stimulations. *J. Immunol.* **192**, 5652–5659 (2014).
30. Fraser, K. A., Schenkel, J. M., Jameson, S. C., Vezys, V. & Masopust, D. Preexisting high frequencies of memory CD8+ T cells favor rapid memory differentiation and preservation of proliferative potential upon boosting. *Immunity* **39**, 171–183 (2013).
31. Thompson, E. A., Beura, L. K., Nelson, C. E., Anderson, K. G. & Vezys, V. Shortened intervals during heterologous boosting preserve memory CD8 T cell function but compromise longevity. *J. Immunol.* **196**, 3054–3063 (2016).
32. Rubin, H. Telomerase and cellular lifespan: ending the debate? *Nat. Biotechnol.* **16**, 396–397 (1998).
33. Mondello, C. et al. Telomere length in fibroblasts and blood cells from healthy centenarians. *Exp. Cell Res.* **248**, 234–242 (1999).
34. Weng, N. P., Levine, B. L., June, C. H. & Hodes, R. J. Regulated expression of telomerase activity in human T lymphocyte development and activation. *J. Exp. Med.* **183**, 2471–2479 (1996).
35. Weng, N., Hathcock, K. S. & Hodes, R. J. Regulation of telomere length and telomerase in T and B cells: a mechanism for maintaining replicative potential. *Immunity* **9**, 151–157 (1998).
36. Hathcock, K. S., Kaech, S. M., Ahmed, R. & Hodes, R. J. Induction of telomerase activity and maintenance of telomere length in virus-specific effector and memory CD8+ T cells. *J. Immunol.* **170**, 147–152 (2003).
37. Callicott, R. J. & Womack, J. E. Real-time PCR assay for measurement of mouse telomeres. *Comp. Med.* **56**, 17–22 (2006).
38. Bally, A. P. R., Austin, J. W. & Boss, J. M. Genetic and epigenetic regulation of PD-1 expression. *J. Immunol.* **196**, 2431–2437 (2016).
39. Duraiswamy, J. et al. Phenotype, function, and gene expression profiles of programmed death-1hi CD8 T cells in healthy human adults. *J. Immunol.* **186**, 4200–4212 (2011).
40. Sekine, T. et al. TOX is expressed by exhausted and polyfunctional human effector memory CD8+ T cells. *Sci. Immunol.* **5**, eaba7918 (2020).
41. Lee, K. et al. Characterization of age-associated exhausted CD8+ T cells defined by increased expression of Tim-3 and PD-1. *Aging Cell* **15**, 291–300 (2016).
42. Bengsch, B. et al. Epigenomic-guided mass cytometry profiling reveals disease-specific features of exhausted CD8 T cells. *Immunity* **48**, 1029–1045 (2018).

Methods

Mice

Donor female B6.SJL-Ptprc^{a}Pepc^{b}/BoyJ (CD45.1^{+} B6) and P14 CD8^{+} T cell transgenic mice were bred at the University of Minnesota animal facilities. Female C57BL/6J (CD45.2^{+} B6) mice were purchased from Jackson Laboratories and served as recipient mice, which were 8–10 weeks old at the time of first infection. Animals were housed with cycles of 14 h of light and 10 h of dark. Their environment was maintained at temperatures between 68 and 72 °F and humidity levels of 30–70%. Animals were treated according to the Institutional Animal Care and Use Committee guidelines and the protocols were approved by the Institutional Animal Care and Use Committee at the University of Minnesota.

Viral infections

CD45.1^{+} tertiary memory cells were expanded through heterologous prime–boost–boost infection with 10^6 plaque-forming units (p.f.u.) VSVnj, an experiment-specific period of rest, 2×10^6 p.f.u. VVn, an experiment-specific period of rest, and 10^7 p.f.u. of VSVind. Following transfer to recipient CD45.2^{+} mice, cells were expanded through heterologous prime–boost–boost infection with 10^6 p.f.u. of VSVind, an experiment-specific period of rest, 2×10^6 p.f.u. VVn, an experiment-specific period of rest, and 10^7 p.f.u. VSVnj. All heterologous prime–boost–boost infections were delivered through the tail vein. For LCMV Armstrong infections, 2×10^5 p.f.u. was delivered through an intraperitoneal injection. For LCMV clone 13, mice were given 200 μg of anti-mouse CD4 (GK1.5) from BioXCell through an intraperitoneal injection one day before and one day after an infection through the tail vein with 2×10^6 p.f.u. of virus.

Tracking of ISTCs

At various time points post infections, blood was collected from the submandibular vein. Red blood cells were lysed using ACK lysis buffer, and blood cells were stained with a variety of antibodies that always included anti-mouse CD8a (53-6.7; 1:100) from BD Biosciences, anti-mouse CD44 (IM7; 1:200) from BioLegend, anti-mouse CD45.1 (A20; 1:400), Ghost Dye Red 780 (1:1,000) from Tonbo Biosciences, and major histocompatibility complex I tetramer with the H2Kb-binding RGYVYQGL peptide from VSVind nucleoprotein (N-tetramer; 1:200). Major histocompatibility complex tetramers were prepared as previously described[43]. Flow cytometry data were collected on a BD LSR II, BD Fortessa or Cytek Aurora and analysed using BD FlowJo. After a cell transfer, values for ISTCs were calculated on the basis of the number of cells transferred and 10% survival whereas values for endogenous cells were based on the reported number of naive H2K^{b}/RGYVYQGL-binding cells in B6 mice[44].

Fluorescence-activated cell sorting and cell transfers

A single-cell suspension was prepared from the spleen and macroscopic lymph nodes of donor mice. In some cases, red blood cells were lysed with ACK lysis buffer before the samples were stained with surface antibodies. In other cases, CD8^{+} T cells were enriched through negative selection before they were stained with surface antibodies. CD8^{+} T cell enrichment was carried out using the Stem Cell EasySep Mouse CD8^{+} T Cell Isolation Kit following the manufacturer's instructions or using a prepared cocktail of biotinylated antibodies. Briefly, single-cell suspensions were resuspended at 10^8 cells per millilitre in phosphate-buffered saline (Gibco) supplemented with 2% heat-inactivated fetal bovine serum (Peak Serum) and 1 mM EDTA (Promega) and then incubated with 5% rat serum (Stem Cell) and 0.0275 mg ml^{-1} anti-mouse CD4 (GK1.5) from Invitrogen and anti-mouse CD19 (1D3), anti-mouse CD11b (M1/70), anti-mouse NK1.1 (PK136), anti-mouse F4/80 (BM8.1), anti-mouse TER119, anti-mouse CD45R (RA3-6B2), anti-mouse LY6G (GR1) and anti-mouse CD16/32 (2.4G2) from Tonbo Biosciences. All antibodies were conjugated to biotin. After antibody incubation, antibody-bound cells were removed using the Stem Cell EasySep Mouse Streptavidin RaphidSpheres Isolation kit following the manufacturer's instructions. Cells were then stained with anti-mouse CD8a (53-6.7; 1:200) from BD Biosciences, anti-mouse CD45.1 (A20; 1:200), anti-mouse CD45.2 (104; 1:200), N-tetramer (1:200) and Ghost Dye Red 780 (1:1,000) from Tonbo Biosciences. Live CD8a^{+}VSV-N-tetramer^{+}CD45.1^{+}CD45.2^{-} cells were sorted on a BD FACS Aria II, and 10^5 sorted cells were transferred through the tail vein into recipient mice. Infections resumed the following day.

Quantitative-PCR-based measurement of mouse telomere length

Telomere length was measured using quantitative PCR, including the primers (synthesized by Integrated DNA Technologies) and control gene as described previously[37]. Data were collected using the QuantStudio 5 system (Applied Biosystems). Isolated *M. spretus* DNA was purchased from Jackson Laboratories to serve as a source of mouse DNA with relatively short telomeres.

CellTrace Violet labelling of cells

The cells of a single-cell suspension of cells isolated from the spleen and macroscopic lymph nodes were labelled with CellTrace Violet (Invitrogen) following the manufacturer's instructions. CellTrace Violet-labelled cells were transferred into mice through the tail vein.

RNA-seq

Bulk RNA was isolated from 10^5 sorted cells using the Qiagen RNeasy Plus Micro kit following the manufacturer's instructions. Libraries were prepared using the Takara/Clontech Stranded Total RNA-seq pico input mammalian kit. Naive, 1°, 3° and 27° cells were prepared using kit version 1 and all other samples were prepared used kit version 2. Samples prepared with kit version 1 were sequenced on an Illumina HiSeq; samples prepared with kit version 2 were sequenced on the Illumina NovaSeq 6000. Quality of fastq files was assessed with FastQC. Adapters and low-quality segments were trimmed with Trimmomatic. Filtered reads were aligned to the mouse genome GRCm38 using Hisat2 and the count matrix was generated using featureCounts. All subsequent gene expression data analyses were carried out in the R software. Genes expressed at low levels were filtered using the filterByExpr function and TMM-normalized in edgeR. Differentially expressed genes were determined using limma. The RNA-seq samples were sequenced in two batches. Genes were considered significantly different if log[fold change] > 1 and false discovery rate < 0.05. Heatmaps were generated with the ComplexHeatmap package. We noticed a batch effect between the first and the second run of RNA-seq samples. However, differential gene expression analysis between the two naive groups revealed only few differentially expressed genes, most being undefined genes or ribosomal genes, indicating that the observed batch effect is not confounding our analysis.

Cell phenotyping through flow cytometry

Phenotyping was carried out on either blood cells or splenocytes that were treated with ACK lysis buffer. Cells were stained extracellularly with various combinations of: anti-mouse CD8a (53-6.7; 1:100), anti-mouse CD4 (GK1.5; 1:1,000), anti-mouse CD45.1 (A20; 1:400), anti-mouse CD122 (TM-β1; 1:100), anti-mouse CD62L (MEL-14; 1:800) and anti-mouse KLRG1 (2F1; 1:200) from BD Biosciences, anti-mouse CD44 (IM7; 1:200), anti-mouse CD38 (90; 1:100), anti-mouse CD45.1 (A20; 1:400), anti-mouse CD28 (E18; 1:100), anti-mouse PD1 (RMP1-30; 1:100), anti-mouse CD200R (OX-110; 1:50) and anti-mouse TIM3 (RMT3-23; 1:100) from BioLegend, anti-mouse CD45.1 (A20; 1:400), anti-mouse CD127 (A7R34) (1:100), anti-mouse CD45.2 (104; 1:200) and Ghost Dye Red 780 (1:1,000) from Tonbo Biosciences and either N-tetramer or the H2Db-binding KAVYNFATM peptide from lymphocytic choriomeningitis virus (GP33-tetramer), fixed and permeabilized using Tonbo Foxp3/Transcription Factor Staining Kit, and then stained intracellularly in Tonbo Permeabilization buffer with anti-mouse TOX (TXRX10; 1:50), and

anti-mouse EOMES (Dan11mag; 1:50) from Invitrogen, anti-mouse BCL-2 (10C4; 1:50) from eBioscience, and anti-mouse TCF1/TCF7 (C63D9; 1:50) from Cell Signaling Technology. Flow cytometry data were collected on either a BD Fortessa or Cytek Aurora and analysed with BD FlowJo.

ATAC-seq

ATAC-seq was carried out following a previously described protocol[45]. Library preparation on transposed DNA was carried out with a Nextera DNA library preparation kit following the manufacturer's instructions. Samples were sequenced on an Illumina HiSeq. FastQC was used to assess the quality of fastq files. Reads were aligned to the mouse Genome (UCSC version mm10) using bowtie2 with valid alignment per read and allowed numbers of mismatches set to 1. Samtools was used to generate sorted bam files that contain mapped reads alone, and Picard was used to mark duplicates. All subsequent data analyses were carried out in the R software. Blacklist regions and mitochondrial reads were removed before peak regions were called with csaw using a window width of 200 base pairs. Windows were considered enriched over background if the $\log_2$[fold change] was >3. As biological sample groups strongly differed in the enrichment of reads within accessible chromatin over background, log[c.p.m.] TMM-scaled peak counts were quantile-normalized as previously described[46]. Differential accessibility analysis was carried out with limma, and peak regions were subsequently merged with a maximum distance between adjacent windows of 200 base pairs. Genomic regions were plotted using Gviz.

PD1 methylation analysis

Genomic DNA was isolated from the purified cells and subjected to bisulfite treatment using the Zymo EZ DNA methylation kit as per the manufacturer's instructions. Bisulfite-modified DNA was PCR-amplified using PD1 promoter-specific primers[47]. The amplicon was cloned into TA vector and transformed into bacteria. Vector from individual colonies was sequenced and analysed using the BISMA software (Bremen, Germany), as previously described[47].

In vitro cytokine stimulation

Blood cells were collected from the submandibular vein, red blood cells were lysed using ACK lysis buffer, and cells were resuspended in RPMI supplemented with 5% heat-inactivated fetal bovine serum, 2 mM L-glutamine, 100 U ml^{-1} penicillin–streptomycin and 0.05 mM β-mercaptoethanol. Cells were added to the wells of a 96-well plate and medium containing brefeldin A from Tonbo Biosciences and various concentrations of RGYVYQGL VSV-N peptide synthesized by New England Peptide Inc (now named Vivitide) to yield a final concentration of 3 μM brefeldin A and labelled concentrations of peptide. After 4–5 h, cells were stained extracellularly with anti-mouse CD8a (53-6.7; 1:100) from BD Biosciences, anti-mouse CD45.1 (A20; 1:400), anti-mouse CD45.2 (104; 1:400) and Ghost Dye Red 780 (1:1,000) from Tonbo Biosciences and N-tetramer (1:200), fixed and permeabilized using Tonbo Foxp3/Transcription Factor Staining Kit, and then stained intracellularly in Tonbo Permeabilization buffer with TNF (MP6-XT22; 1:100) from BD Biosciences and IFNγ (XMG1.2; 1:100) from BioLegend. Flow cytometry data were collected on a BD Fortessa and analysed with BD FlowJo software.

Listeria protection

One day after transfer of 10^5 specified sorted N-specific cells, mice were injected through the tail vein with 7×10^3 colony-forming units of *L. monocytogenes* expressing VSV-N (LM-N). Five days after LM-N infection, spleens were removed and cells were lysed through homogenization in sterile 0.5% Igepal CA-630 (Sigma Aldrich). Various dilutions of cell homogenate were plated onto Petri dishes with BBL Brain Heart Infusion Agar (BD Biosciences) prepared according to the manufacturer's instructions, incubated at 37 °C overnight and colonies were counted the next day.

Non-lymphoid tissue analysis

Non-lymphoid tissues were treated as previously described[48], including the use of 3 μg of an intravascular anti-CD8a antibody (53-6.7) from BD Biosciences as previously described[49] to prepare a single-cell suspension. Single-cell suspensions from each tissue were stained extracellularly with anti-mouse CD8a (53-6; 1:00) from BD Biosciences, anti-mouse CD45.1 (A20; 1:200) and Ghost Dye Red 780 (1:1,000) from Tonbo Biosciences, anti-mouse CD69 (H1.2F3; 1:50) from Invitrogen and N-tetramer (1:200). Flow cytometry data were collected on a BD Fortessa and analysed with BD FlowJo software.

Data measurements

Cells that were tracked over time were measured repeatedly after different infections with discreet measurements made on populations of cells within different mice.

Statistical methods

No statistical test was used to determine sample sizes. Mice were randomly assigned to different experimental groups. Researchers were not blinded to experimental groups. Specific statistical tests used to determine significance, group sizes (n) and P values are provided in the figure legends. P value < 0.05, significant. All statistical analysis was carried out using Prism (GraphPad).

Reporting summary

Further information on research design is available in the Nature Portfolio Reporting Summary linked to this article.

Data availability

The data that support the findings of this study are available from the corresponding author upon reasonable request. Sequencing data are available through GEO (accession number GSE213230). Source data are provided with this paper.

43. Altman, J. D. & Davis, M. M. MHC-peptide tetramers to visualize antigen-specific T cells. *Curr. Protoc. Immunol.* **115**, 17.3.1–17.3.44 (2016).
44. Obar, J. J., Khanna, K. M. & Lefrançois, L. Endogenous naive CD8+ T cell precursor frequency regulates primary and memory responses to infection. *Immunity* **28**, 859–869 (2008).
45. Buenrostro, J. D., Wu, B., Chang, H. Y. & Greenleaf, W. J. ATAC-seq: a method for assaying chromatin accessibility genome-wide. *Curr. Protoc. Mol. Biol.* **109**, 21.29.1–21.29.9 (2015).
46. Künzli, M. et al. Long-lived T follicular helper cells retain plasticity and help sustain humoral immunity. *Sci. Immunol.* **5**, eaay5552 (2020).
47. Youngblood, B. et al. Chronic virus infection enforces demethylation of the locus that encodes PD-1 in antigen-specific CD8+ T cells. *Immunity* **35**, 400–412 (2011).
48. Steinert, E. M. et al. Quantifying memory CD8 T cells reveals regionalization of immunosurveillance. *Cell* **161**, 737–749 (2015).
49. Anderson, K. G. et al. Intravascular staining for discrimination of vascular and tissue leukocytes. *Nat. Protoc.* **9**, 209–222 (2014).

Acknowledgements We thank members of the laboratories of D.M. and V.V. for helpful discussions. We thank the University of Minnesota Flow Cytometry resource for cell sorting (J. Motl, T. Martin and R. Arora). This study was supported by National Institutes of Health grants R01 AI084913, R01 AI146032 (D.M.) and T32HL007741 (A.G.S.), and Swiss National Science Foundation grant P2BSP3_200187 (M.K.).

Author contributions A.G.S., M.K., C.F.Q., M.C.S., L.S., J.L. and H.E.G. carried out the experiments, analysed data and prepared visualizations. B.Y. analysed data and prepared visualizations. D.Z. created and shared reagents. A.G.S., M.K., V.V. and D.M. designed the experiments and wrote the manuscript.

Competing interests The authors declare no competing interests.

Additional information

Supplementary information The online version contains supplementary material available at https://doi.org/10.1038/s41586-022-05626-9.

Correspondence and requests for materials should be addressed to David Masopust.

Peer review information *Nature* thanks Susan Kaech and the other, anonymous, reviewer(s) for their contribution to the peer review of this work.

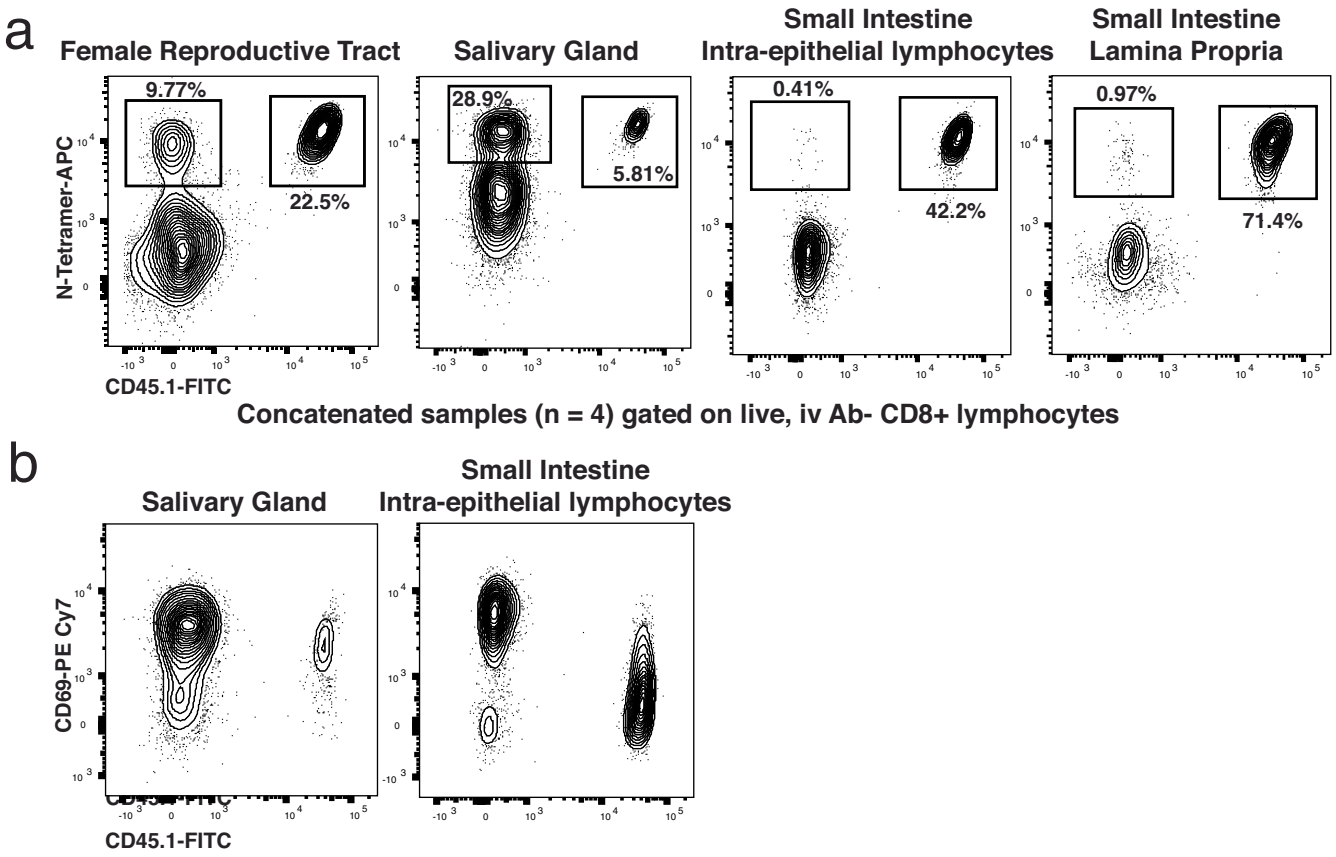

Extended Data Fig. 1 | Iteratively stimulated T cells populate non-lymphoid tissues. a) CD45.1+ 48° ISTC memory CD8 T cells were transferred to naïve mice, followed by three heterologous prime-boost-boost immunizations. Non-lymphoid tissues were analyzed 48 days after the 51° boost. Flow cytometry plots are gated on live CD8a+ lymphocytes that were not stained by intravascular in vivo antibody labeling. b) CD69 expression on endogenous 3° cells (CD45.1-) and 48° memory CD8 T cells (CD45.1+). Plots concatenated from four mice and experiment is representative of three similar experiments with similar results.

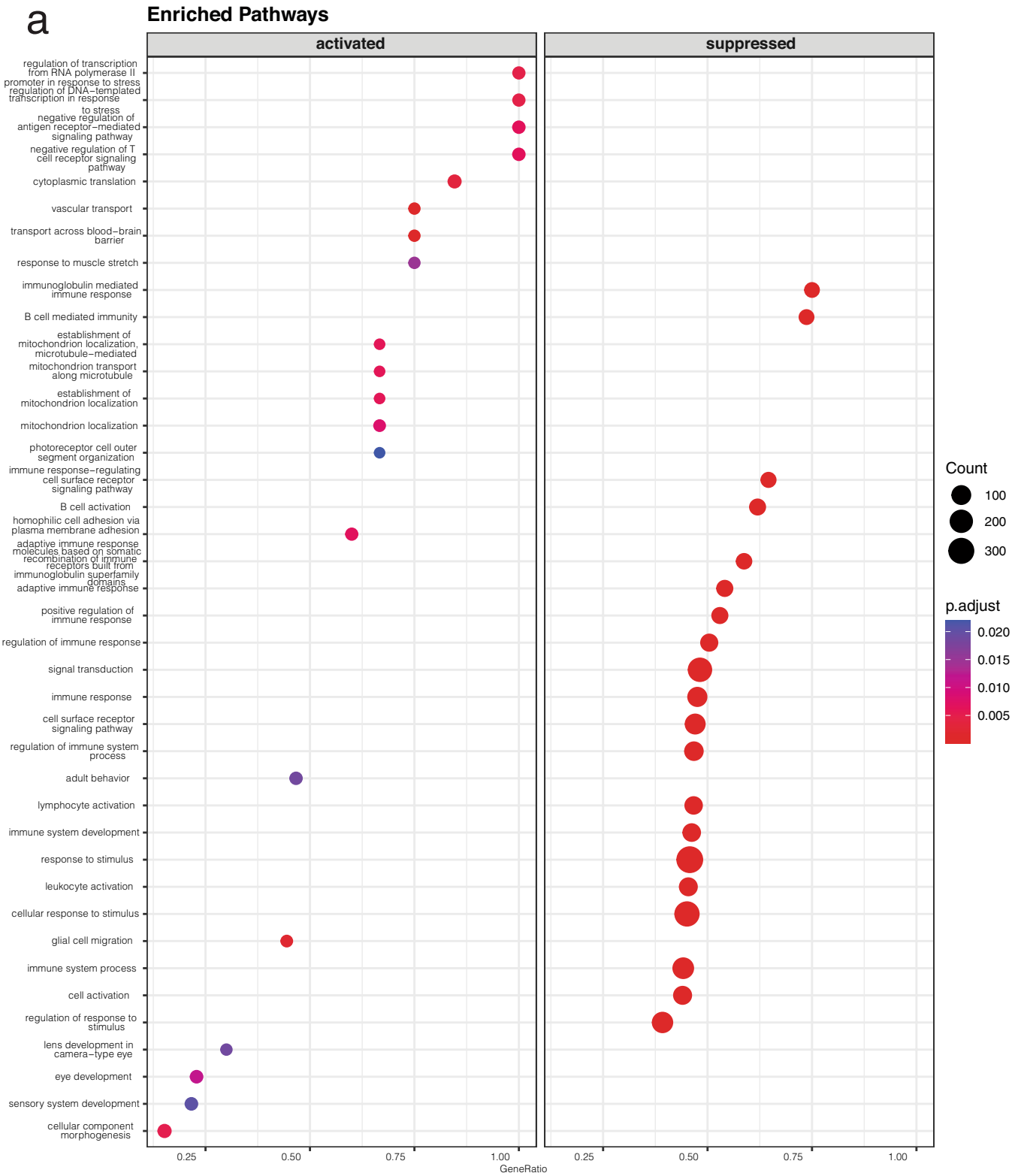

Extended Data Fig. 2 | Gene set enrichment analysis of iteratively stimulated CD8 T cells. Gene set enrichment analysis was performed on differentially expressed genes between 45° ISTCs and primary memory cells using the category "Biological process" of the Gene Ontology database. The top 20 upregulated (activated) and top 20 downregulated (suppressed) pathways in ISTCs are shown. Statistical significance was determined using Over-Representation analysis.

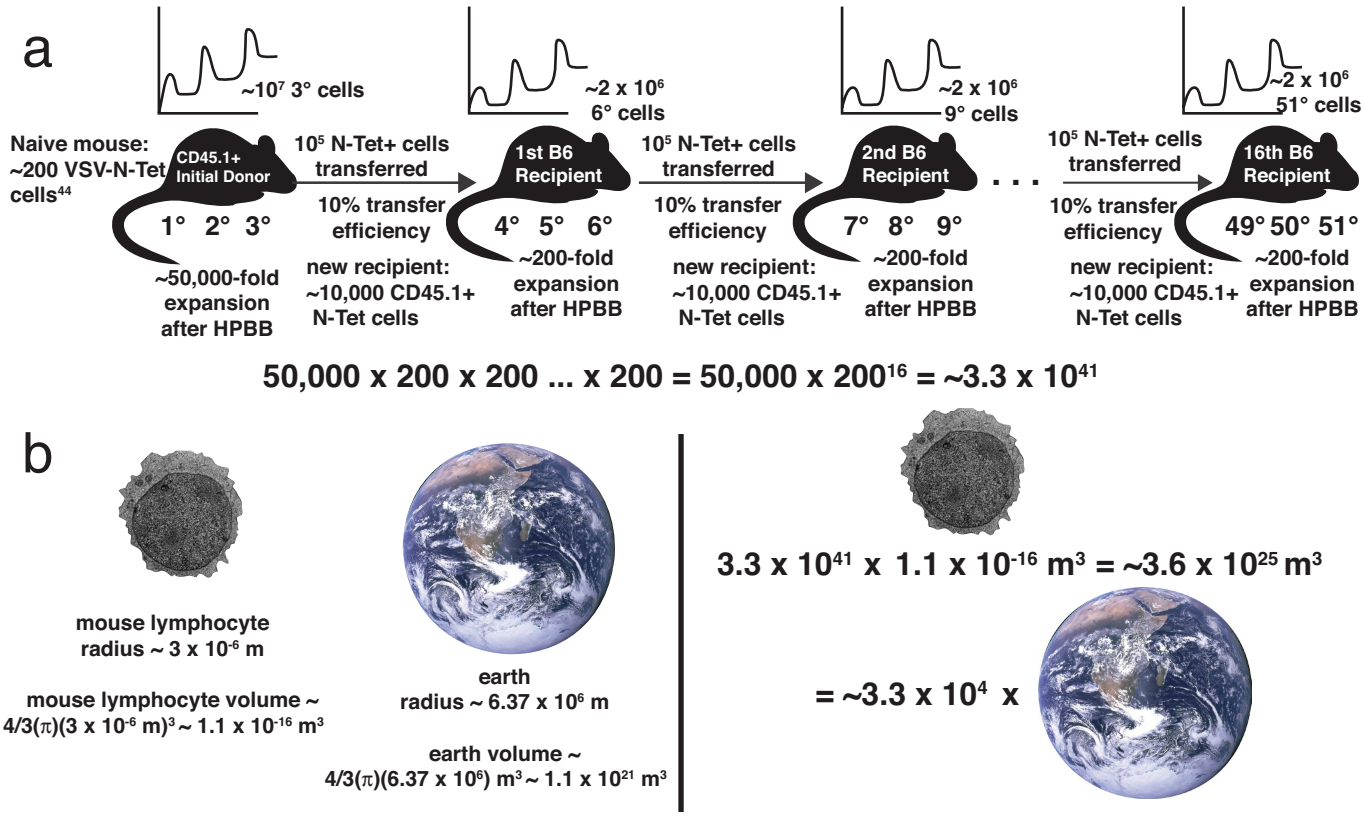

Extended Data Fig. 3 | A single naïve CD8 T cell shows the potential to produce >10^{40} memory cell progeny. a) Schematic showing estimate of cell expansion potential after 51 HPBB immunizations. HPBB: three successive Heterologous Prime, Boost, Boost immunizations. b) Schematic comparing the volume of earth with the theoretical volume of memory T cells implied by the calculated proliferation potential of a naïve CD8 T cell.

nature portfolio

Corresponding author(s): David Masopust

Last updated by author(s): Nov 17, 2022

Reporting Summary

Nature Portfolio wishes to improve the reproducibility of the work that we publish. This form provides structure for consistency and transparency in reporting. For further information on Nature Portfolio policies, see our Editorial Policies and the Editorial Policy Checklist.

Statistics

For all statistical analyses, confirm that the following items are present in the figure legend, table legend, main text, or Methods section.

n/a	Confirmed
☐	☒ The exact sample size (*n*) for each experimental group/condition, given as a discrete number and unit of measurement
☐	☒ A statement on whether measurements were taken from distinct samples or whether the same sample was measured repeatedly
☐	☒ The statistical test(s) used AND whether they are one- or two-sided *Only common tests should be described solely by name; describe more complex techniques in the Methods section.*
☒	☐ A description of all covariates tested
☐	☒ A description of any assumptions or corrections, such as tests of normality and adjustment for multiple comparisons
☐	☒ A full description of the statistical parameters including central tendency (e.g. means) or other basic estimates (e.g. regression coefficient) AND variation (e.g. standard deviation) or associated estimates of uncertainty (e.g. confidence intervals)
☐	☒ For null hypothesis testing, the test statistic (e.g. *F*, *t*, *r*) with confidence intervals, effect sizes, degrees of freedom and *P* value noted *Give P values as exact values whenever suitable.*
☒	☐ For Bayesian analysis, information on the choice of priors and Markov chain Monte Carlo settings
☒	☐ For hierarchical and complex designs, identification of the appropriate level for tests and full reporting of outcomes
☒	☐ Estimates of effect sizes (e.g. Cohen's *d*, Pearson's *r*), indicating how they were calculated

Our web collection on statistics for biologists contains articles on many of the points above.

Software and code

Policy information about availability of computer code

Data collection	Flow ctyometry was collected using either BD Biosciences' FACSDiva or Cytek's SpectroFlo software. The most recent versions used were FACSDiva v. 8.01 and SpectroFlo v. 3.0.1 qPCR data was collected using Thermo Fisher's QuantStudio Design and Analytics Software v.1.4.3
Data analysis	Flow cytometry data was analyzed using BD Biosciences' FlowJo, most recently v. 10.8.1 Statistical analysis and data presentation was done using Graphpad's Prism, most recently v. 9.4.1 Next Generation Sequencing analysis used: FastQC v0.11.7 Trimmomatic v0.33 Hisat2 v2.1.0 featureCounts v2.12.0 EdgeR v3.36.0 filterByExpr (part of EdgeR) Limma v3.50.3 ComplexHeatmap v2.10.0 bowtie2-2.4.2 Samtools-1.4.1-0 Picard 2.25.6 Csaw 1.28.0 Gviz 1.38.4

RStudio 2022.02.3
R 4.1.3

For manuscripts utilizing custom algorithms or software that are central to the research but not yet described in published literature, software must be made available to editors and reviewers. We strongly encourage code deposition in a community repository (e.g. GitHub). See the Nature Portfolio guidelines for submitting code & software for further information.

Data

Policy information about availability of data

All manuscripts must include a data availability statement. This statement should provide the following information, where applicable:

- Accession codes, unique identifiers, or web links for publicly available datasets
- A description of any restrictions on data availability
- For clinical datasets or third party data, please ensure that the statement adheres to our policy

Sequencing alignment relied on mouse genome mm10 - GRCm38 : https://www.ncbi.nlm.nih.gov/assembly/GCF_000001635.20/

Gene expression was compared to the expression of genes in exhausted T cells using GSE41867: https://www.ncbi.nlm.nih.gov/geo/query/acc.cgi?acc=GSE41867

The data that support the findings of this study are available from the corresponding author upon reasonable request. Sequencing data is available via GEO (accession number: GSE213230).

Human research participants

Policy information about studies involving human research participants and Sex and Gender in Research.

Reporting on sex and gender	N/A
Population characteristics	N/A
Recruitment	N/A
Ethics oversight	N/A

Note that full information on the approval of the study protocol must also be provided in the manuscript.

Field-specific reporting

Please select the one below that is the best fit for your research. If you are not sure, read the appropriate sections before making your selection.

☒ Life sciences ☐ Behavioural & social sciences ☐ Ecological, evolutionary & environmental sciences

For a reference copy of the document with all sections, see nature.com/documents/nr-reporting-summary-flat.pdf

Life sciences study design

All studies must disclose on these points even when the disclosure is negative.

Sample size	No statistical test was used to determine sample sizes. Group size was determined based on previous experience and expected results.
Data exclusions	No data were excluded from analysis.
Replication	Data presented in figure 1 were repeated 2-4 times with generally similar results. Data in subsequent figures come from the longest running cohort of cells. RNA-seq and ATAC-seq experiments were performed on samples that were collected from independent animals at independent time points then sequenced in either 1 (ATAC-seq) or 2 (RNA-seq) sequencing runs. All other experiments were performed ≥ 2 times with similar results.
Randomization	Mice were randomly assigned to different experimental groups.
Blinding	Researchers were not blinded to experimental groups. Data presented is quantitative and did not rely on qualitative assessments.

Reporting for specific materials, systems and methods

We require information from authors about some types of materials, experimental systems and methods used in many studies. Here, indicate whether each material, system or method listed is relevant to your study. If you are not sure if a list item applies to your research, read the appropriate section before selecting a response.

Materials & experimental systems

n/a	Involved in the study
☐	☒ Antibodies
☒	☐ Eukaryotic cell lines
☒	☐ Palaeontology and archaeology
☐	☒ Animals and other organisms
☒	☐ Clinical data
☒	☐ Dual use research of concern

Methods

n/a	Involved in the study
☒	☐ ChIP-seq
☐	☒ Flow cytometry
☒	☐ MRI-based neuroimaging

Antibodies

Antibodies used

Target Fluorochrome Manufacturer Clone Lot Dilution
CD44 AlexaFluor 700 BioLegend IM7 B332765 1:200
CD38 AlexaFluor 700 BioLegend 90 B364980 1:100
CD8a APC eBioscience 53-6.7 E07057-1634 1:100
CD8a BUV395 BD Biosciences 53-6.7 2026422 1:100
CD4 BUV496 BD Biosciences GK1.5 1182277 1:1000
CD4 BUV737 BD Biosciences GK1.5 9304790 1:1000
CD4 BV786 BD Biosciences GK1.5 4227537 1:1000
CD45.1 BUV737 BD Biosciences A20 9595 1:400
CD62L BUV737 BD Biosciences MEL-14 1315770 1:800
CD122 BV421 BD Biosciences TM-b 1 7278969 1:100
Tim-3 BV421 BioLegend RMT3-23 B337501 1:100
CD45.1 BV421 BioLegend A20 B198259 1:400
TNFa BV421 BD Biosciences MP6-XT22 2143828 1:100
CD44 BV510 BioLegend IM-7 B311963 1:400
Tim-3 BV605 BioLegend RMT3-23 B340648 1:100
CD8a BV650 BD Biosciences 53-6.7 5149600 1:200
KLRG1 BV711 BD Biosciences 2F1 1194048 1:200
CD44 BV785 BioLegend IM-7 B215593 1:200
Tox eFluor 660 Invitrogen TXRX10 2151328 1:50
CD45.1 FITC Tonbo Biosciences A20 C0453070920354 1:400
Blc2 FITC eBioscience 10C4 E14007-104 1:100
CD200R FITC BioLegend OX-110 B241589 1:50
Dead Ghost Dye Red780 Tonbo Biosciences D0865031422133 1:1000
CD127 PE Tonbo Biosciences A7R34 C1271080320503 1:100
TCF1/TCF7 PE Cell Signaling Technologies C63D9 8 1:50
IL-2 PE eBioscience JES6-5H4 4324650 1:100
CD28 PE Cy7 BioLegend E18 B216064 1:100
eomes PE Cy7 Invitrogen Dan11mag 1995327 1:50
CD69 PE Cy7 Invitrogen H1.2F3 2138816
PD-1 PE Cy7 BioLegend RMP1-30 B335007 1:100
IFNg PE Cy7 BioLegend XMG1.2 B367890 1:100
CD45.2 PE Cy7 Tonbo Biosciences 104 C0454040921603 1:200
CD4 Biotin Invitrogen RM4-5 2083934 1:400
CD19 Biotin Tonbo Biosciences 1D3 C0193052520304 1:400
CD11b Biotin Tonbo Biosciences M1/70 C0112012422304 1:400
NK1.1 Biotin Tonbo Biosciences PK136 C5941061719304 1:400
F4/80 Biotin Tonbo Biosciences BM8.1 C4801052021304 1:400
Ter119 Biotin Tonbo Biosciences TER-119 C5921032422304 1:400
CD45R Biotin Tonbo Biosciences RA3-6B2 C0452012722304 1:400
Ly-6G Biotin Tonbo Biosciences RB6-8C5 C5931011922304 1:400
CD16/32 Biotin Tonbo Biosciences 2.4G2 C0161031220304 1:400

Validation

All antibodies used are commercially available. Validation can be found at manufacturers websites:
Target Fluorochrome Manufacturer Clone Validation
CD44 AlexaFluor 700 BioLegend IM7 https://www.biolegend.com/en-us/products/alexa-fluor-700-anti-mouse-human-cd44-antibody-3406
CD38 AlexaFluor 700 BioLegend 90 https://www.biolegend.com/en-us/products/alexa-fluor-700-anti-mouse-cd38-antibody-20599
CD8a APC eBioscience 53-6.7 https://www.thermofisher.com/antibody/product/CD8a-Antibody-clone-53-6-7-Monoclonal/17-0081-81
CD8a BUV395 BD Biosciences 53-6.7 https://www.bdbiosciences.com/en-us/products/reagents/flow-cytometry-reagents/research-reagents/single-color-antibodies-ruo/buv395-rat-anti-mouse-cd8a.563786
CD4 BUV496 BD Biosciences GK1.5 https://www.bdbiosciences.com/en-us/products/reagents/flow-cytometry-reagents/research-

reagents/single-color-antibodies-ruo/buv496-rat-anti-mouse-cd4.612952
CD4 BUV737 BD Biosciences GK1.5 https://www.bdbiosciences.com/en-us/products/reagents/flow-cytometry-reagents/research-reagents/single-color-antibodies-ruo/buv737-rat-anti-mouse-cd4.612761
CD4 BV786 BD Biosciences GK1.5 https://www.bdbiosciences.com/en-us/products/reagents/flow-cytometry-reagents/research-reagents/single-color-antibodies-ruo/bv786-rat-anti-mouse-cd4.563331
CD45.1 BUV737 BD Biosciences A20 https://www.bdbiosciences.com/en-us/products/reagents/flow-cytometry-reagents/research-reagents/single-color-antibodies-ruo/buv737-mouse-anti-mouse-cd45-1.612811
CD62L BUV737 BD Biosciences MEL-14 https://www.bdbiosciences.com/en-us/products/reagents/flow-cytometry-reagents/research-reagents/single-color-antibodies/buv737-rat-anti-mouse-cd62l.612833
CD122 BV421 BD Biosciences TM-b 1 https://www.bdbiosciences.com/en-us/products/reagents/flow-cytometry-reagents/research-reagents/single-color-antibodies-ruo/bv421-rat-anti-mouse-cd122.752988
Tim-3 BV421 BioLegend RMT3-23 https://www.biolegend.com/en-us/products/brilliant-violet-421-anti-mouse-cd366-tim-3-antibody-13392
CD45.1 BV421 BioLegend A20 https://www.biolegend.com/en-us/products/brilliant-violet-421-anti-mouse-cd45-1-antibody-7255
TNFa BV421 BD Biosciences MP6-XT22 https://www.bdbiosciences.com/en-us/products/reagents/flow-cytometry-reagents/research-reagents/single-color-antibodies-ruo/bv421-rat-anti-mouse-tnf.563387
CD44 BV510 BioLegend IM7 https://www.biolegend.com/en-us/products/brilliant-violet-510-anti-mouse-human-cd44-antibody-7994
Tim-3 BV605 BioLegend RMT3-23 https://www.biolegend.com/en-us/products/brilliant-violet-605-anti-mouse-cd366-tim-3-antibody-13391
CD8a BV650 BD Biosciences 53-6.7 https://www.bdbiosciences.com/en-us/products/reagents/flow-cytometry-reagents/research-reagents/single-color-antibodies-ruo/bv650-rat-anti-mouse-cd8a.563234
KLRG1 BV711 BD Biosciences 2F1 https://www.bdbiosciences.com/en-us/products/reagents/flow-cytometry-reagents/research-reagents/single-color-antibodies-ruo/bv711-hamster-anti-mouse-klrg1.564014
CD44 BV785 BioLegend IM-7 https://www.biolegend.com/en-us/products/brilliant-violet-785-anti-mouse-human-cd44-antibody-7959
Tox eFluor 660 Invitrogen TXRX10 https://www.thermofisher.com/antibody/product/TOX-Antibody-clone-TXRX10-Monoclonal/50-6502-82
CD45.1 FITC Tonbo Biosciences A20 https://tonbobio.com/products/fitc-anti-mouse-cd45-1-a20
Blc2 FITC eBioscience 10C4 https://www.thermofisher.com/antibody/product/Bcl-2-Antibody-clone-10C4-Monoclonal/11-6992-42
CD200R FITC BioLegend OX-110 https://www.biolegend.com/en-us/products/fitc-anti-mouse-cd200r-ox2r-antibody-5174
Dead Ghost Dye Red780 Tonbo Biosciences https://tonbobio.com/products/ghost-dye-red-780
CD127 PE Tonbo Biosciences A7R34 https://tonbobio.com/products/pe-anti-mouse-cd127-il-7ra-a7r34
TCF1/TCF7 PE Cell Signaling Technology C63D9 https://www.cellsignal.com/products/antibody-conjugates/tcf1-tcf7-c63d9-rabbit-mab-pe-conjugate/14456?site-search-type=Products&N=4294956287&Ntt=c63d9&fromPage=plp
IL-2 PE eBioscience JES6-5H4 https://www.thermofisher.com/antibody/product/IL-2-Antibody-clone-JES6-5H4-Monoclonal/12-7021-82
CD28 PE Cy7 BioLegend E18 https://www.biolegend.com/en-us/products/pe-cyanine7-anti-mouse-cd28-antibody-3780
eomes PE Cy7 Invitrogen Dan11mag https://www.thermofisher.com/antibody/product/EOMES-Antibody-clone-Dan11mag-Monoclonal/25-4875-82
CD69 PE Cy7 Invitrogen H1.2F3 https://www.thermofisher.com/antibody/product/CD69-Antibody-clone-H1-2F3-Monoclonal/25-0691-82
PD-1 PE Cy7 BioLegend RMP1-30 https://www.biolegend.com/en-us/products/pe-cyanine7-anti-mouse-cd279-pd-1-antibody-3612
IFNg PE Cy7 BioLegend XMG1.2 https://www.biolegend.com/en-us/products/pe-cyanine7-anti-mouse-ifn-gamma-antibody-5865
CD45.2 PE Cy7 Tonbo Biosciences 104 https://tonbobio.com/products/pe-cyanine7-anti-mouse-cd45-2-104
CD4 Biotin Invitrogen RM4-5 https://www.thermofisher.com/antibody/product/CD4-Antibody-clone-RM4-5-Monoclonal/13-0042-82
CD19 Biotin Tonbo Biosciences 1D3 https://tonbobio.com/products/biotin-anti-mouse-cd19-1d3
CD11b Biotin Tonbo Biosciences M1/70 https://tonbobio.com/products/biotin-anti-human-mouse-cd11b-m1-70
NK1.1 Biotin Tonbo Biosciences PK136 https://tonbobio.com/products/biotin-anti-mouse-nk1-1-cd161-pk136
F4/80 Biotin Tonbo Biosciences BM8.1 https://tonbobio.com/products/biotin-anti-mouse-f4-80-antigen-bm8-1
Ter119 Biotin Tonbo Biosciences TER-119 https://tonbobio.com/products/biotin-anti-mouse-ter-119-ter-119
CD45R Biotin Tonbo Biosciences RA3-6B2 https://tonbobio.com/products/biotin-anti-human-mouse-cd45r-b220-ra3-6b2
Ly-6G Biotin Tonbo Biosciences RB6-8C5 https://tonbobio.com/products/biotin-anti-mouse-ly-6g-gr-1-rb6-8c5
CD16/32 Biotin Tonbo Biosciences 2.4G2 https://tonbobio.com/products/biotin-anti-mouse-cd16-cd32-2-4g2

Animals and other research organisms

Policy information about studies involving animals; ARRIVE guidelines recommended for reporting animal research, and Sex and Gender in Research

Laboratory animals	Donor female B6.SJL-PtprcaPepcb/BoyJ (CD45.1+ B6) and P14 CD8 T-cell transgenic mice were bred at the University of Minnesota animal facilities and were used at 6-16 weeks. Female C57BL/6J (CD45.2+ B6) mice were purchased from Jackson Laboratories and served as recipient mice at age 6-16 weeks. Animals were housed with cycles of 14 hours of light and 10 hours of dark. Their environment was maintained at temperatures between 68 and 72 degrees Fahrenheit and humidity levels between 30-70%.
Wild animals	Wild animals were not used in this experiment
Reporting on sex	Because sorted cells were transferred between donor and recipient mice, experiments were restricted to females.
Field-collected samples	Field-collected samples were not used in this study.
Ethics oversight	Animals were treated according to the Institutional Animal Care and Use Committee guidelines.

Note that full information on the approval of the study protocol must also be provided in the manuscript.

Flow Cytometry

Plots

Confirm that:

☒ The axis labels state the marker and fluorochrome used (e.g. CD4-FITC).

☒ The axis scales are clearly visible. Include numbers along axes only for bottom left plot of group (a 'group' is an analysis of identical markers).

☒ All plots are contour plots with outliers or pseudocolor plots.

☒ A numerical value for number of cells or percentage (with statistics) is provided.

Methodology

Sample preparation	Blood was collected from the submandibular vein. Red blood cells were lysed using ACK lysis buffer. A single cell suspension was prepared from the spleen and macroscopic lymph nodes of donor mice. In some cases, red blood cells were lysed with ACK lysis buffer before the samples were stained with surface antibodies. In other cases, CD8+ T cells were enriched via negative selection before they were stained with surface antibodies. Phenotyping was done on either blood cells or splenocytes that were treated with ACK lysis buffer. Non-lymphoid tissues were treated as previously described, including the use of an intravascular anti-CD8a antibody (53-6.7) from BD Biosciences as previously described.
Instrument	Data was collected on a BD LSR II, BD Fortessa, BD Fortessa X-20, BD Fortessa X-30, or Cytek Aurora (3-laser). Cell sorting was done using a BD FACSAria II.
Software	BD FlowJo was used for all analysis. Most recently, version 10.8.1
Cell population abundance	Post Sort analysis was routinely performed on sorted samples and the target population was above 95% of total events and ~100% of cells in a FSC-A/SSC-A lymphocyte gate.
Gating strategy	Singlets were gated using FSC-H/FSC-A then SSC-A/SSC-H. In some experiments, outliers were removed by gating off of extreme events in at least one channel per laser. With the exception of figure 4a, dead cells were removed with a viability stain. Lymphocytes were gated on FSC-A by SSC-A. CD8a+ cells were gated as CD8a+/CD4-. Total N-Tet+ cells were gated as CD44 low to high/N-Tetramer+. Naive cells were gated as CD44 low/N-Tet-. Endogenous N-Tet cells were gated as N-Tet+/CD45.1-. Transferred congenic cells were gated as N-Tet+/CD45.1+.

☒ Tick this box to confirm that a figure exemplifying the gating strategy is provided in the Supplementary Information.